Preparation of alkaline PVA-based polymer electrolytes for Ni–MH and Zn–air batteries

C-C. YANG* and S-J. LIN
Department of Chemical Engineering, Ming-Chi Institute of Technology, Taipei, Taiwan, R.O.C
*(*author for correspondence, e-mail: ccyang@ccsun.mit.edu.tw)*

Abstract

Alkaline PVA polymer electrolyte with high ionic conductivity of about 0.047 S cm^{-1} at room temperature was obtained by a solution casting method. The PVA polymer electrolytes, blended with KOH and H$_2$O, were studied by DSC, TGA, cyclic voltammetric and a.c. impedance methods. The PVA polymer electrolytes show good mechanical strength and high ionic conductivity. The electrochemical stability window at the metal–electrolyte interface is ±1.2 V for stainless steel. Ni–MH and Zn–air batteries with PVA polymer electrolytes were assembled and tested. Experimental results show good electrochemical performances of the PVA-based Ni–MH and Zn–air batteries.

1. Introduction

Solid polymer electrolytes (SPEs) have been extensively studied in recent years for application in many electrochemical devices such as cellular phones, thin credit cards and laptop computers [1]. A polymer electrolyte consisting of polymer matrix, plasticizers, and alkali metal salts, and solvents [1–4]. Solid polymer electrolyte (SPE) must be free of solvent. Although a SPE can form a dimensionally stable film, its ambient temperature conductivity is low; in the range of 10^{-7}–10^{-8} S cm^{-1}. It is too low for application in electrochemical devices. To enhance the conductivity, several approaches have been suggested [4]. Polymer blends, polymer modified with a plasticizer or a mixture of solvents, as well as gel electrolytes have been explored. The main goal of these studies is to obtain films with a high fraction of amorphous phase, which exhibits a much higher conductivity than the crystalline phase.

Some studies have focused on PEO-based polymer electrolytes with lithium salts and organic solvents. The lithium polymer system appears to be the most widely studied due to its potential application in high energy density batteries. There are few literature data on alkaline solid polymer electrolytes based on the PEO–KOH system [5–8]. Lewandowski et al. [9] studied the PVA–KOH polymer electrolyte system by AC impedance and cyclic voltammetric methods. It was found that the ionic conductivity of the PVA–KOH–H$_2$O (~40 wt% of PVA, 25–30 wt% of KOH, and 30–35 wt% of H$_2$O) polymer electrolyte is of the order of 10^{-3}–10^{-4} S cm^{-1}, and E_a is at the level of 22–28 kJ mol^{-1}. In this investigation, we report the preparation and properties of an alkaline electrolyte based on the PVA polymer. The ionic conductivity of the polymer films was measured by a.c. impedance spectroscopy. The electrochemical stability window was examined by cyclic voltammetry. The amorphous microstructure was analysed in terms of the glass transition temperature (T_g) measured by DSC. The thermal stability was examined by TGA.

In general, PVA alkaline polymer electrolytes can be applied in all-solid alkaline batteries. Two alkaline batteries, (Ni–MH and Zn–air batteries) have been selected to study the performance of PVA polymer electrolyte. The major application of the Ni–MH battery demands high energy and power density sources for portable devices, such as cellular and computer products. A solid-state polymer Ni–MH battery is a good candidate for future applications. A Zn–air cell also has been selected to test the electrical performance of the PVA polymer electrolyte. Zn–air batteries [10–15] possess the highest specific energy, compared with other Zn-based alkaline batteries. This is due to the unlimited and free supply of oxygen from the atmosphere. Also, there are many advantages in Zn–air batteries, which include a stable working voltage, a higher energy density which is independent of load and temperature, longer dry storage time, and use of environmentally friendly and low cost active materials. Alkaline PVA polymer electrolytes were applied to both Ni–MH and Zn–air types. The electrochemical properties of the solid-state polymer Ni–MH and Zn–air batteries were evaluated under galvanostatic discharge conditions.

2. Experimental details

PVA (Aldrich), and KOH (Merck) were used as received without further purification. The degree of polymerization and saponification of PVA were 1700 and 98–99%, respectively. The alkaline polymer electrolyte films were prepared by the solution casting method. The appropriate weight ratios of the PVA and KOH were dissolved in water. The solution was stirred continuously until the solution mixture took on a homogeneous viscous liquid appearance. The resulting homogeneous solution was poured onto a petri dish and weighed immediately and then the excess water was allowed to evaporate slowly. After evaporation, the petri dish with the film was weighed again. The composition of polymer electrolyte was determined from the mass balance. The thickness of the films was controlled at between 0.30 and 0.60 mm. Conductivity measurements were made for the polymer electrolyte film by an a.c. two-terminal method. The polymer sample films were sandwiched between SS304 stainless steel, ion-blocking electrodes, each of surface area 0.785 cm^2, in a spring-loaded glass holder. A thermocouple was positioned close to the electrolyte film for temperature measurement. Cyclic voltammetry and a.c. impedance measurements were carried out using an Autolab PGSTAT 30 equipment (Eco Chemie BV, The Netherlands). The a.c. frequency range from 1 MHz to 1 Hz at an excitation signal of 5 mV was recorded. The impedance of the sample film was measured from 20 to 70 °C. Experimental temperatures were maintained within ±0.1 °C by a convection oven.

The DSC thermal analysis was done using a Perkin-Elmer Pyris 7 DSC system. Measurements were carried out by heating from −70 to 200 °C, at a rate of 10 °C min^{-1} in a N_2 atmosphere with about 5–10 mg sample. The TGA thermal analysis was conducted using a Perkin-Elmer Pyris 7 TGA system. Measurements were carried out by heating from 25 to 600 °C, under nitrogen atmosphere at a rate of 10 °C min^{-1} with a 5–10 mg sample.

Pasted nickel electrodes were made of $Ni(OH)_2$ powder, acetylene black, and PTFE binder. A 2 cm × 2 cm nickel-foam sheet was used as the substrate, and a Ni wire was spot-welded on the top edge as the terminal. The $Ni(OH)_2$ powder, acetylene black, CoO and PTFE binder were mixed in the proportion of 70 wt % $Ni(OH)_2$, 15 wt % acetylene black, 10 wt % CoO and 5 wt % PTFE. The solid mixture was mixed with IPA solvent to form a paste. The paste was filled into a nickel-foam substrate, dried at 110 °C for 1 h, then pressed under 1 ton cm^{-2} pressure. The $Ni(OH)_2$ electrode was immersed in 32% KOH solution for 24 h in an open cell for testing. The metal-hydride electrode was a commercially available AB$_5$ type alloy. The capacity of the electrode is limited by the $Ni(OH)_2$ electrode. The activated $Ni(OH)_2$ or MH electrode was used as working electrode. The electrolyte for activation was aqueous 32% KOH solution. A platinum screen and a mercury oxide electrode (HgO/Hg/6 M KOH) were used as counter electrode and reference electrode, respectively. The alkaline PVA polymer electrolyte was sandwiched between the activated $Ni(OH)_2$ electrode and the activated MH electrode for 24 h in a closed cell. Several alkaline solid-state Ni–MH cells were charged for 7.5 h at $C/5$, kept for 30 min at open circuit, and then discharged at different rates to 0.8 V. The charge/discharge cycles of the Ni–MH cells were performed at room temperature. The charge/discharge experiments were carried out after the cell reached a stable condition (around 5–6 cycles). The electrochemical characteristics of the Ni–MH cells were examined using the charge/discharge equipment (BAT 778 model).

An air cathode electrode consisted of a diffusion layer, a Ni-foam current collector, and an active layer. The slurry for the gas diffusion layer was prepared using a mixture of 70 wt % Shawinigan acetylene black (AB50) with specific surface area 70 m^2 g^{-1} and 30 wt % PTFE (Teflon-30 suspension) as a wet-proofing agent and binder. The slurry was coated on the Ni-foam substrate (as a current collector), then pressed at 100 kg cm^{-2}. The diffusion layer was initially sintered at a temperature of 300 °C for 30 min. The active layer of the air electrode was then prepared by spraying a mixture of a 15 wt % PTFE, 5–10 wt % $KMnO_4$ or MnO_2, 60 wt % Vulcan XC-72R (with surface area 250 m^2 g^{-1}), and an appropriate amount of IPA onto the gas diffusion layer. The air electrode with the gas diffusion layer and the active layer was finally sintered at 375 °C for 30 min under a pressure of 80 kg cm^{-2}. The thickness of the air electrode was controlled at 0.5–0.6 mm. The Zn gels used as anodes were made according to the following compositions: 67 wt % Zn powder, 1–2 wt % Cabopol gelling agent, 32 wt % KOH, and some oxide additives. A solid-state Zn–air cell with the PVA polymer electrolyte, the air cathode electrode, and Zn gel anode was assembled and tested. The Zn–air cells were discharged at different constant current conditions. The electrochemical characteristics of Zn–air cells were carried out with the BAT 778 model charge/discharge equipment.

3. Results and discussion

The DSC curves of pure PVA and PVA-KOH systems are shown in Figure 1. An endothermic peak of pure PVA is observed at 225 °C, which corresponds to the melting temperature of PVA, as shown in Table 1.

Two exothermic peaks for PVA–KOH–H_2O system are observed at 62 °C and 210 °C, which may correspond to solvent evaporation and recrystallization of PVA. It can be seen that the melting temperature of PVA, T_m, disappears when KOH was added to the PVA–KOH polymer system. The disappearance of T_m for PVA polymer electrolyte indicated a change from a crystalline phase to an amorphous phase. It was observed that the PVA polymer was in an amorphous state when the KOH was added. The ionic conductivity of the polymer electrolyte is due to transport of cations
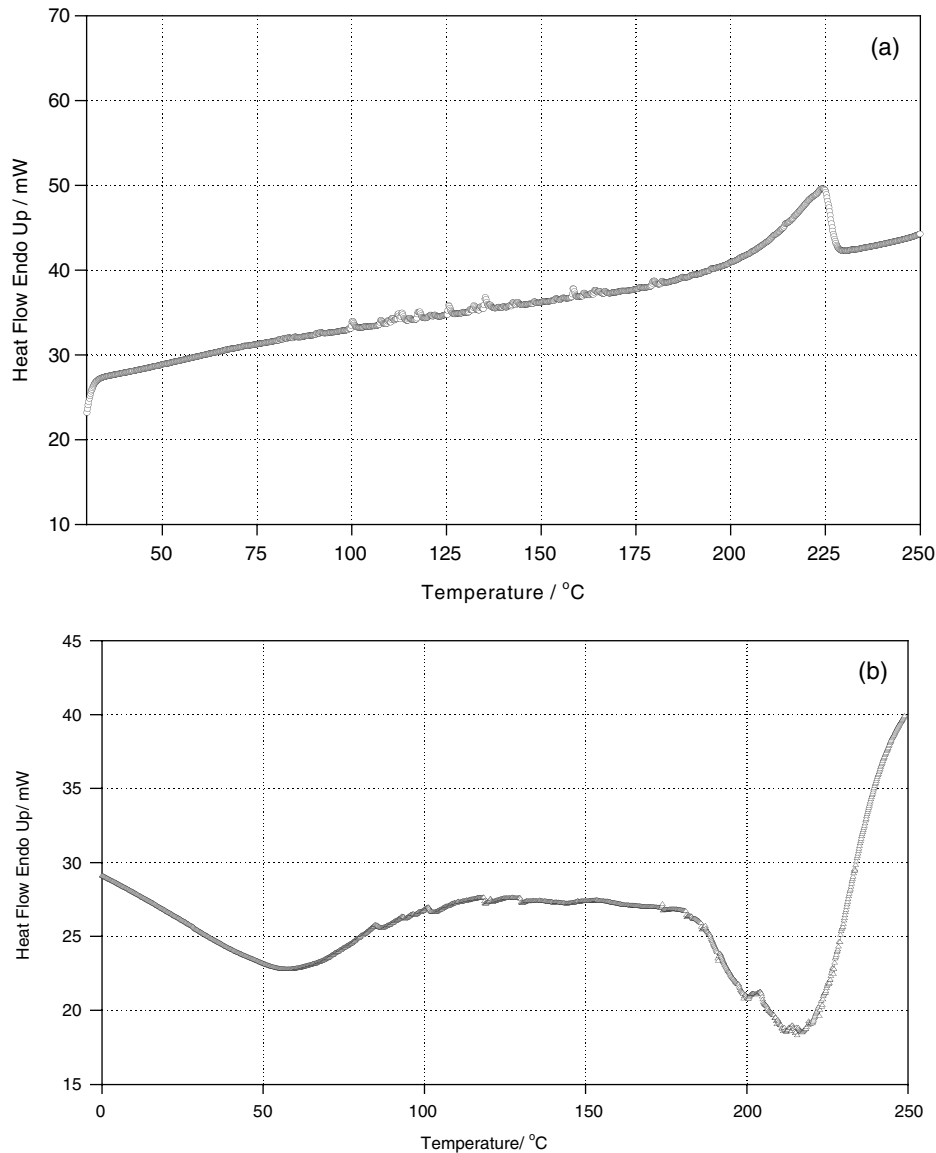
Fig. 1. DSC thermographs for PVA polymer electrolyte (a) Pure PVA; (b) PVA–KOH–H$_2$O electrolyte (30:30:40 in wt%).

Table 1. Conductivity values and thermal properties of polymer electrolytes

Properties	Polymer electrolyte	
	PEO-based	PVA-based /PVA:KOH:H$_2$O (30:30:40 in wt %)
σ/S cm^{-1} at 25 °C	10^{-7}–10^{-8}	0.047
E_a/kJ mol^{-1}	20–30	3.83
T_g/°C	−62.01	–
T_m/°C	61.17	–

* T_g = −62.69 °C, T_m = 61 °C for PEO polymer; T_g = 86.60 °C and T_m = 210 °C for PVA polymer.

and anions in the polymer matrix. It is known that the ionic mobility is increased by segmental motion of the polymer host, and the ionic conductivity is mainly localized to the amorphous phase. The segment motion occurs more readily in the amorphous polymer backbone. The mechanism of ionic transport in the polymer electrolytes is still not clear.

The thermograph curves for PVA–KOH–H$_2$O system are shown in Figure 2. There is a weight loss of 73% at a temperature of 262 °C for the pure PVA polymer. The PVA–KOH polymer electrolyte presents a multiple step degradation, which begins in the region between 60 °C and 200 °C with a 20% loss of weight. Subsequently, there is a 25% weight loss when the temperature is changed from 200 °C to 400 °C, finally there is a total weight loss of 73% when the temperature reaches 600 °C. It was found that the thermal stability of PVA–KOH polymer electrolyte has been degraded when KOH is added. The PVA–KOH polymer electrolyte starts to lose weight at 60 °C, and the decomposition temperature of PVA polymer electrolyte is also reduced to 220 °C, compared to 275 °C for pure PVA polymer.

The typical a.c. impedance spectra for the alkaline polymer electrolyte film PVA–KOH–H$_2$O system is
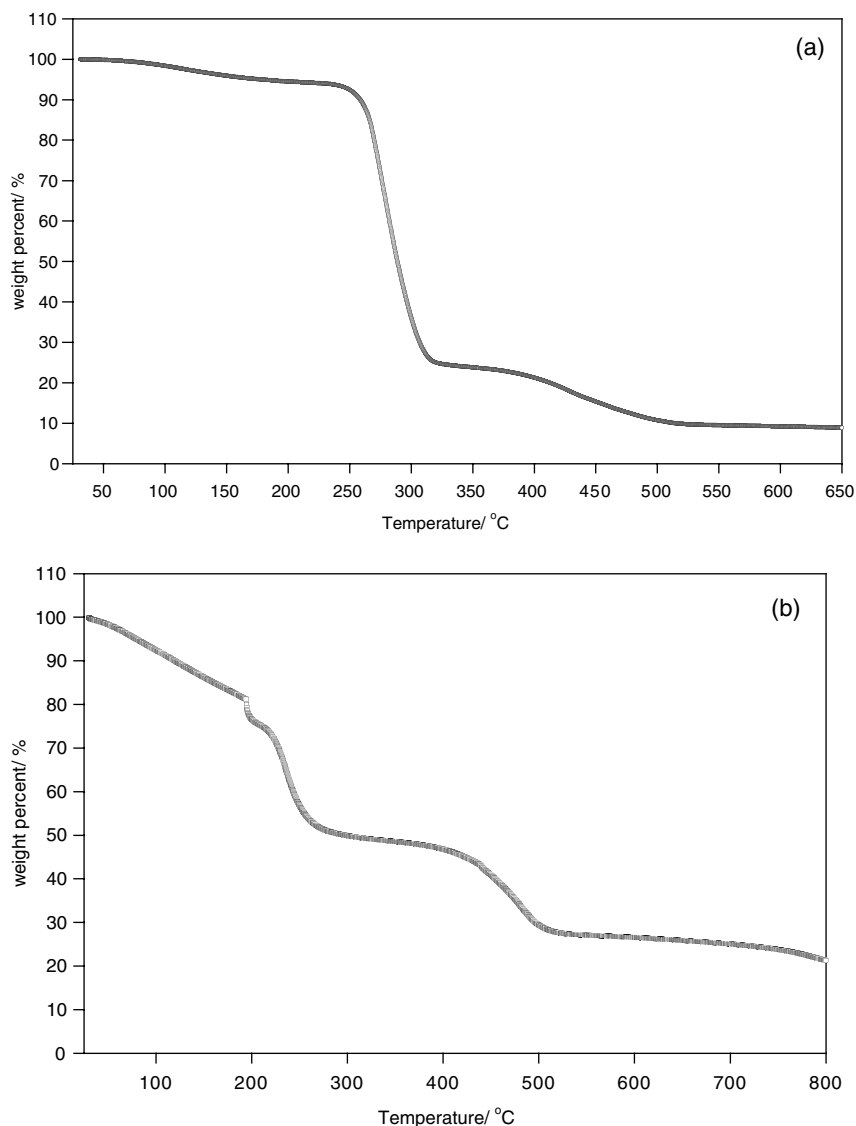
Fig. 2. TGA thermographs for PVA polymer electrolyte (a) Pure PVA; (b) PVA–KOH–H$_2$O electrolyte (30:30:40 in wt%).

shown in Figure 3. The a.c. spectra show a typical non-vertical spike for blocking electrodes, that is, SS |PVA SPE| SS cell. Analysis of the spectra yields information about the properties of the electrolyte such as bulk resistance, R_b. Taking into account the thickness of the electrolyte films, the R_b value was converted into the electrolyte conductance, σ, according to the formula: $\sigma(\text{S cm}^{-1}) = \ell(\text{cm})/R_b(\text{ohm}) \times A(\text{cm}^2)$. Typically, the R_b values for the PVA–KOH films are of the order of 1 to 5 ohm and are highly dependent on the contents of KOH and H$_2$O in the films. The corresponding values of ionic conductivities are at the level of 10^{-2} S cm^{-1}. The a.c. impedance spectra for PVA–KOH–H$_2$O electrolyte films containing various compositions of KOH were obtained at room temperature; typical impedance spectra for several weight ratios of PVA polymer electrolytes are shown in Figure 4. Table 2 shows the conductivity values of PVA polymer electrolytes with different compositions.

The temperature dependence of the conductivity is of the Arrhenius type: $\sigma = \sigma_o = \exp(-E_a/RT)$. The linear plots of $\log_{10}(\sigma)$ against $1/T$, as shown in Figure 5, give the activation energy (E_a), which is dependent on the KOH content. The E_a for PVA–KOH–H$_2$O (30:40:30 in wt %) film is 3.83 kJ mol^{-1}, whereas the value for the electrolyte film with the PVA–KOH–H$_2$O (40:40:20 in wt %) system is 15.42 kJ mol^{-1}. It was observed that the lowest activation energy is a characteristic for electrolyte films of the highest conductivity.

High conductivity is not enough to make the polymer electrolyte suitable for practical battery applications. A broad electrochemical stability window is important for practical use of these films. The cyclic voltammetric analysis sweeping in the −1.5 V to +1.5 V range for the alkaline PVA SPE and different separators soaked with KOH is shown in Figure 6. The stability of the PVA polymer electrolyte at the interface with the stainless steel as electrode is limited by the potentials of about +1.2 V on the anodic side and of −1.2 V at the cathodic side, which gives a window of about 2.4 V. It is apparent that the PE/PP and cellulose separators soaked with KOH show a much narrower electrochemical stability
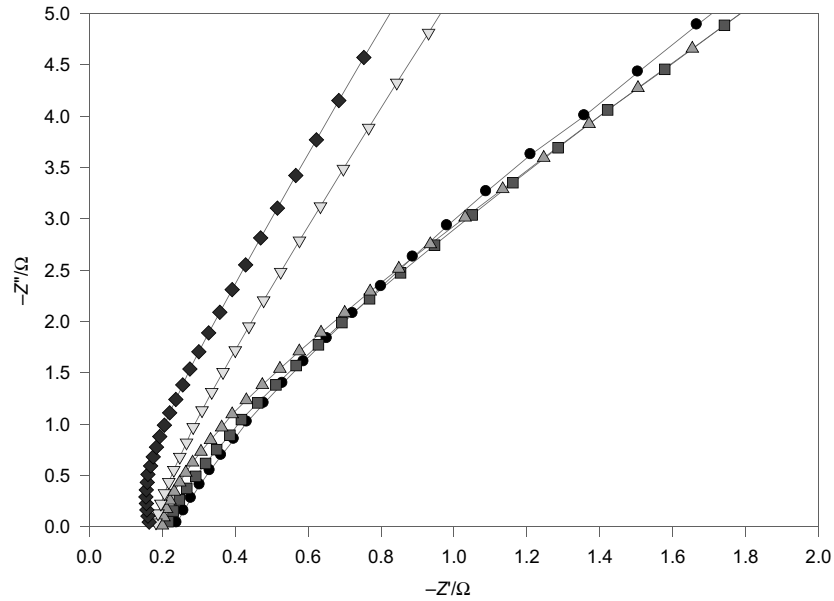
Fig. 3. A.c. impedence spectra for PVA polymer electrolysis at different temperatures (PVA–KOH–H$_2$O 30:30:40 in wt%); (●) at 25 °C, R_b = 0.239 Ω, (■) at 40 °C, R_b = 0.210 Ω; (▲) at 50 °C, R_b = 0.206 Ω; (▽) at 60 °C, R_b = 0.190 Ω; (◆) at 70 °C, R_b = 0.173 Ω.
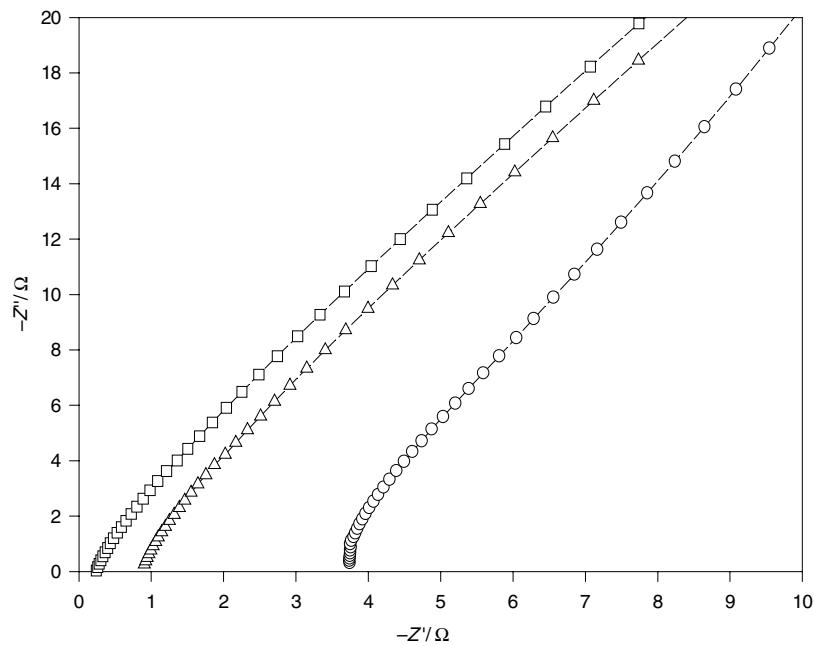

Fig. 4. A.c. impedence spectra for PVA SPE with different compositions (○) PVA:KOH:H$_2$O = 40:40:20; (□) PVA:KOH:H$_2$O = 30:30:40; (△) PVA:KOH:H$_2$O = 25:25:50.

Table 2. Conductivity values (S cm^{-1}) of PVA polymer electrolytes at varied compositions at a constant of 50% relative humidity (RH)

T/°C	PVA:KOH:H$_2$O (30:40:30 in wt%)	PVA:KOH:H$_2$O (40:40:20 in wt%)
30	0.0471	0.0187
40	0.0499	0.0233
50	0.0528	0.0269
60	0.0560	0.0324
70	0.0570	0.0490

window than that of PVA SPE, as shown in Figure 6. Alkaline PVA polymer electrolyte demonstrates good mechanical strength and electrochemical stability.

A solid-state Ni–MH cell shows a charge voltage plateau value of 1.38 V and a discharge voltage of 1.25 V. After finishing the 10 charge/discharge cycle tests, the capacity density of Ni(OH)$_2$ active material had an average of 250 mAh g^{-1}. The capacity of a solid-state Ni–MH cell is limited by the Ni(OH)$_2$ positive electrode. The average current efficiency is 83% after 10 cycle tests. The average percentage utilization is around 82%. The theoretical capacity density of Ni(OH)$_2$ is 289 mAh g^{-1},
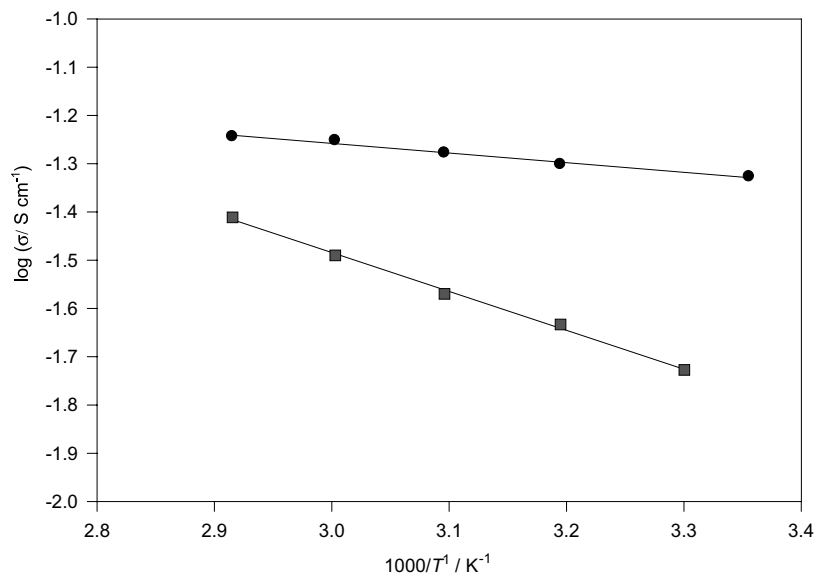
Fig. 5. Arrhenius plot for PVA polymer electrolytes at different compositions; ($\bullet$) PVA:KOH:H$_2$O = 30:40:30 in wt %, E_a = 3.83 kJ mol^{-1}; ($\blacksquare$) PVA:KOH:H$_2$O = 40:40:20 in wt %, E_a = 15.42 kJ mol^{-1}.
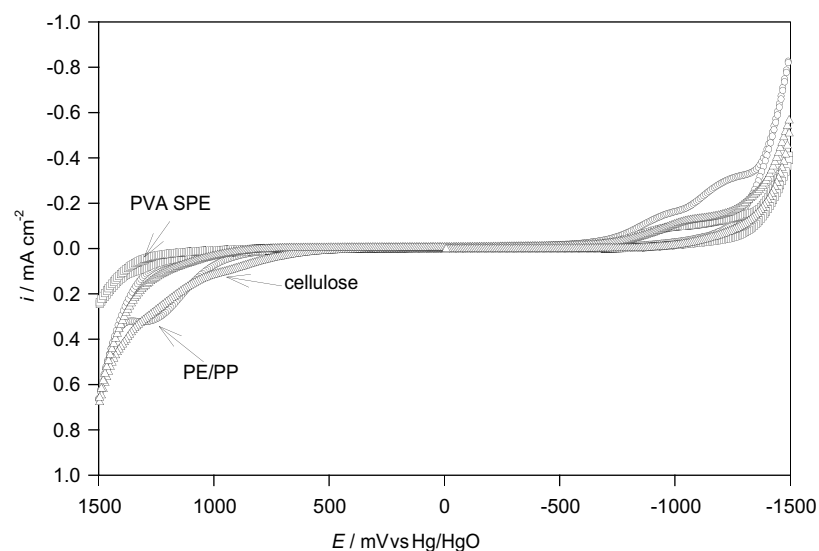
Fig. 6. Cyclic voltammetric analysis results for PVA SPE, PE/PP and cellulose separators. ($\bigcirc$) PE/PP separator; ($\square$) PVA polymer electrolytes; ($\triangle$) cellulose separator.

which is based on the one electron transfer reaction of $Ni(OH)_2 + OH^- \rightarrow NiOOH + H_2O + e^-$.

The discharge curves of Zn–air cells with the PVA polymer electrolyte and different types of separators are shown in Figure 7. The Zn–air cell with PVA polymer electrolyte exhibits the highest capacity of 1475 mAh (theoretical capacity: 1600 mAh, percentage of utilization: 92%). The percents utilization for conventional Zn-air batteries with PE/PP and cellulose separators are only 49.5% and 57%, respectively. Experimental results for Zn–air cells are listed in Table 3. The reason for solid-state Zn–air cell having higher the capacity density and the percentage utilization is due to having smaller pore sizes with the dimension of 0.1–0.2 μm, compared with that of PE/PP separator. In contrast, the conventional Zn–air cell using PE/PP or cellular separator

having a much larger pore size (with dimension of 10–20 μm) is move easily short circuited at a high discharge rate. It was also found that there was a non uniform pore size distribution within the PE/PP and cellulose separators. The discharge curves of Zn–air cells with the PVA SPE at various discharge rates are shown in Figure 8. The percent of utilization for Zn gels is about 82–92% at various discharge rates (from $C/5$ to $C/20$), as listed in Table 4.

4. Conclusions

Alkaline PVA SPE was obtained by a solution casting method. The characteristic properties of PVA-based polymer electrolytes were studied by DSC, TGA, cyclic
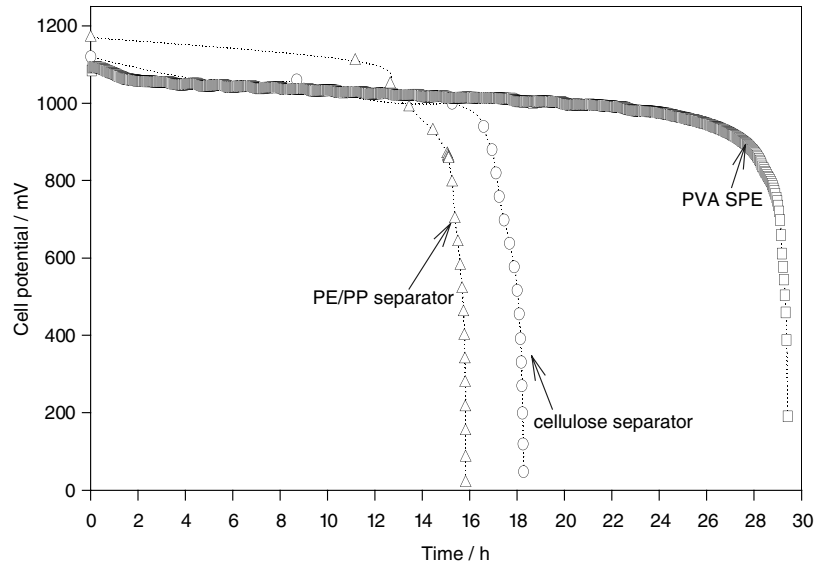
Fig. 7. Discharge curves for Zn–air cells with different types of separators and PVA polymer electrolyte. Discharge current 50 mA; Q_{th} = 1600 mAh; (□) PVA polymer electrolyte; (△) PB/PP separator; (○) cellulose separator.

Table 3. Experimental results for different Zn–air cells at a constant discharge rate
(Cell dimension: 2 cm × 3 cm, A = 6 cm^2).

Properties	Zn–air with PE/PP separator	Zn–air with cellulose separator	Zn–air with PVA SPE
Theo. capacity/mAh	1,600	1,600	1,600
Discharge current/mA	50	50	50
Discharge time/h	15.8	18.2	29.5
Real capacity/mAh	792	915	1475
Utilization/%	49.50	57.20	92.20

voltammetric and a.c. impedance methods. The ionic conductivities of alkaline PVA polymer electrolyte films was measured at various temperatures. The highest ionic conductivity at room temperature is about 0.047 S cm^{-1}. It was experimentally observed that the thermal stability of PVA polymer electrolyte was degraded when KOH was added. Alkaline PVA polymer electrolytes show good mechanical strength and electrochemical stability. The activation energy (E_a) for PVA–KOH–H$_2$O system is of the order of 4 to 15 kJ mol^{-1}; and depends on the composition of
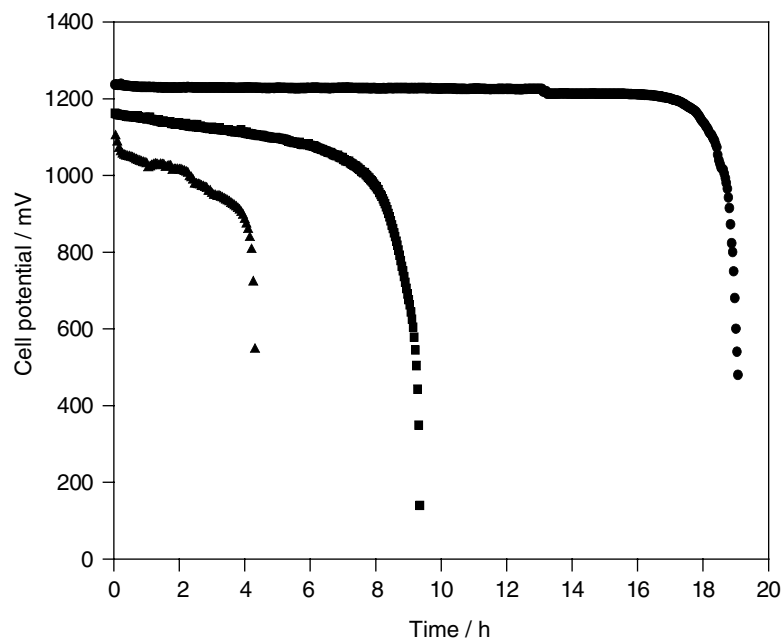

Fig. 8. Discharge curves for solid-state Zn–air cells at different discharge rates. (Q_{th} = 1560 mAh; PVA–KOH–H$_2$O = 30:30:40 in wt%). (▲) $C/5$; (■) $C/10$; (●) $C/20$.

Table 4. Experimental results of PVA polymer Zn–air cells at varied discharge rates
(Cell dimension: 2 cm × 3 cm, $A = 6$ cm^2).

Properties	Discharge rates		
	C/5	*C*/10	*C*/20
Theo. capacity/mAh	1560	1560	1560
Discharge current/mA	300	150	75
Discharge time/h	4.31	9.35	19.08
Real capacity/mAh	1293	1402.5	1431
Utilization/%	82.88	89.90	91.37

KOH. Solid-state Ni–MH and Zn–air batteries using PVA SPE were assembled and examined. Results indicate that both solid-state Ni–MH and Zn–air cells show good electrochemical properties of charge/discharge characteristics. Alkaline PVA-based polymer electrolyte shows a potential for application in alkaline battery systems.

Acknowledgement

References

1. F.M. Gray, 'Solid Polymer: Electrolytes: Fundamental and Technological Application' (VCH, New York, 1991).
2. D.E. Fenton, J.M. Parker and P.V. Wright, *Polymer* **14** (1973) 589.
3. P.V. Wright, *Brit. Polymer J.* **7** (1975) 319.
4. M.B. Armand, J.M. Chabagno and M.J. Duclot, *in* M.J. Duclot, P. Vashishta, J.M. Mundy, G.K. Shenoy (Eds), 'Fast Ion Transport in Solids' (1979).
5. J.F. Fauvarque, S. Gunot, N. Bouzir, E. Salmon and J.F. Penneau, *Electrochim. Acta* **40** (1995) 2449.
6. S. Gunot, E. Salmon, J.F. Penneau and F. Fauvarque, *Electrochim. Acta* **43** (1998) 1163.
7. N. Vassal, E. Salmon and F. Fauvarque, *Electrochim. Acta* **45** (2000) 1527.
8. N. Vassal, E. Salmon and J.F. Fauvarque, *J. Electrochem. Soc.* **146** (1999) 20.
9. A. Lewandowski, K. Skorupska and J. Malinska, *Solid State Ionics* **133** (2000) 265.
10. S-I. Pyun and Y.G. Ryu, *J. Power Sources* **62** (1996) 1.
11. C-C. Chang, T-C. Wen and H-J. Tien, *Electrochim. Acta* **42** (1997) 557.
12. D.B. Zhou and H.V. Poorten, *Electrochim. Acta* **40** (1995) 1819.
13. E. Passalacqua, G. Squadrito, F. Lufrano, A. Patti and L. Giorgi, *J. Appl. Electrochem.* **31** (2001) 449.
14. Z. Wei, W. Huang, S. Zhang and J. Tan, *J. Power Sources* **91** (2000) 83.
15. R. Othman, W.J. Basirun, A.H. Yahaya and A.K. Arof, *J. Power Sources* **103** (2001) 34.